Journal of Petroleum Research & Studies

The Geomechanics and the Acoustic Anisotropy of Reservoir Rocks

Ahmed Zarzor Al-Yaseri*; Mohammed Al –Humairi, Rodrigo Borda*****

***Petroleum Dep. University of Baghdad , Iraq ;**

**** University of Messan , Iraq ;**

***** University of Oklahoma, USA**

Abstract

Knowing the mechanical properties (Young's modulus (E)) , Poisson's Ratio (ν), Shear Modulus (G), Bulk modulus (K) and compressibility which is the inverse of Bulk modulus) of the rocks involve in a reservoir, are critical factors for reservoir characterization). Those properties affect a wide variety of applications into the petroleum industry; from drilling well planning and execution to production performance (sand production, compaction, subsidence, etc) passing through a wide variety of topics like wellbore stability, well completions and of course reservoir characterization. For these reasons, the knowledge of these properties is really valuable for people working in the petroleum industry and of course working in reservoir characterization.

This study was located in Berea town, Oklahoma, and it was intended to identify the geomechanical and acoustic properties of a sandstone sample. The Berea sandstone elastic properties are characterized using two methods: Quasi static and Dynamic. A detailed explanation of the sample preparation and the testing

procedure is provided. Calculation results for both methods showed consistent values for the Young's modulus being around 3,000,000 psi. The Poisson's Ratio value is between 0.13 and 0.3. This study was performed in the PoroMechanics Institute (PMI) in the Sarkeys Energy Center at the University of Oklahoma, USA.

Monitoring equipment was used to obtain all the information necessary for the proper characterization of the rock. The results of this work are a good tool that can be used in future simulations such as hydraulic fracturing treatment, reservoir fluid flow or reserve estimation.

الخلاصة

ان معرفة الخواص الميكانيكية مثل معامل يونغ ونسبة بواسون و معامل القص وغيرها من الخصائص والتي تؤثر على مجموعة واسعة من التطبيقات في الصناعة النفط مثل حفر الابار و تصنيف المكامن وفي هندسة الانتاج و التكسر الصناعي للطبقات المكمنية.

ان النماذج المدروسة في هذا العمل ماخوذة من مدينة بيريا في ولاية أوكلاهوما الامريكية حيث تم في هذا العمل حساب الخصائص الجيوميكانيكية باستخدام طريقتين هما شبه ثابت وحيوي. ان النتائج كانت متقاربة باستخدم الطريقتين حيث تم تقدير معامل يونغ 3,000,000 رطل و قيمة بواسون بين 0,13 و 0,3

تم إجراء هذه الدراسة في في قسم علوم الارض في جامعة أوكلاهوما في الولايات المتحدة الأمريكية .ان نتائج هذا العمل هي أداة جيدة يمكن استخدامها في المستقبل في هندسة الانتاج والمكامن النفطية.

Introduction

The mechanical properties of rocks are important for reservoir characterization. Elastic parameters of the rock are required to design fracturing treatments. The fluid flow in the reservoir is also a function of the compressibility of the formation and it can be a key parameter for reserves estimation. In this study, the Berea sandstone is characterized by two important elastic properties: the Young's Modulus and the Poisson's ratio. In this study, a rock sample from the Berea sandstone formation located in Berea town – Oklahoma. The first part of this work will go over the quasi-static and dynamic measurements of the vertical sample.

The second part of this work will go over the procedures used during this experiment, including descriptions of the sample, preparation of the sample, and acquisition of the data. The final part of this report will discuss the results and measurements obtained through this experiment.

1.1 Problem Statement and Objectives

Two important parameters to describe the elastic properties of a material are: the ratio of the stress to the strain, "Young's modulus", and the ratio of transverse strain to the axial strain "Poisson's ratio". In the geomechanics lab, there are two methods to determine these elastic properties: The Quasi-static method and the Dynamics method.

The Quasi-static method is the measurement of the strain during the application of load to a core sample.

The dynamic method is the measurement of the velocities of compression and shear waves traveling through the core sample while the load is applied.

The measurements for the quasi static method and the dynamic method were recorded simultaneously while the load was applied to the Berea rock sample. The objective of this study is to calculate the Young Modulus and the Poisson's ratio from the data acquired from these two methods.

1.2 Vertical Direction: Quasi-Static Measurements

As mentioned, the Quasi-Static measurement consists of applying load to a core sample and recording the change in length.

For this purpose, a strain gauge is attached to the side of the core sample. This strain gauge is capable of sensing changes in length.

1.2.1 Force and Stress

Force is the quantification of the interaction of a given body with others. The effect of these forces on a body follow the Newton's law of motion (sum of forces acting on a body is equal to the mass of the body times its acceleration), but due to the fact that in the analysis of rock force could not be assumed acting on a point, the concept of stress tensor should be introduced, which is the variation of the traction (force per unit of area) with orientation (Jaeger et al, 2007).

Stress (σ): is the internal force per unit of area, when the area approaches to zero. To give a complete description of the stress state at a point between a sample; a stress tensor should be defined. The stress tensor is a symmetric second-order tensor, which means that the stress tensor reduce the quantity of stress components that have to be measure from four to three in two dimensional plane and from nine to six in a tridimensional problem (Jaeger et al.).

Two components of the stress tensor should be defined:

Normal stress (σ_{ii}): defined as the component perpendicular to the plane on which it is acting.

Shear stress (σ_{ij} or τ_{ij}): is the component of the stress tangential or parallel to the plane on which it is acting fig(1).

Where the subscript "i" identify the axis normal to the actual surface, and the second subscript "j" identify the direction of the stress (FJ aer et al, 1992) by convention, compression is assumed positive.

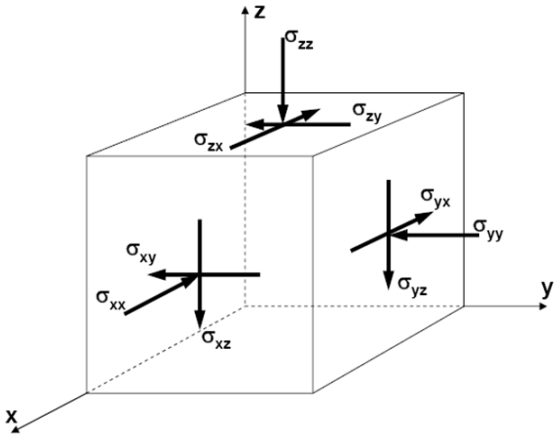

Fig. (1) Graphic representation of the stress tensor (After Geomechanics in integrated reservoir characterization II), MPGE/SGG/SEC Younane Abousleiman, Fall 2009.

$$[\sigma] = \begin{bmatrix} \sigma_{xx} & \sigma_{xy} & \sigma_{xz} \\ \sigma_{yx} & \sigma_{yy} & \sigma_{yz} \\ \sigma_{zx} & \sigma_{zy} & \sigma_{zz} \end{bmatrix}$$

Tridimensional representation of the stress tensor due to its properties, $\sigma_{ij} = \sigma_{ji}$

1.2.2 Displacement and Strain

Displacement is the fundamental kinematic variable in rock mechanics. And the objective in solving a rock mechanics problem is to calculate the displacement vector at every point in the rock, based on knowledge of the applied surface tractions, the body forces, and the boundary conditions. To do this, it is necessary to introduce a set of intermediate quantities known as Strains. The reason is that the stresses are more related to the strains than the displacements themselves.

Strain (ε): is the deformation per unit of length or width. It is a measure of the relative displacement of nearby particles (Jaeger et al.). There are two components of strain:

Normal strain (ε_{ii}): is the deformation per unit of length in the direction of the deformation.

Shear strain (ε_{ij}): is the deformation per unit of length where the length over which the deformation occurs is at right angle to the direction of the deformation. (Coates, 1981) or in other words, is the measure of the angular distortion, rather than stretching (Jaeger et al.)

The strain tensor is a symmetric second-order tensor too represented by:

$$[\varepsilon] = \begin{bmatrix} \varepsilon_{xx} & \varepsilon_{xy} & \varepsilon_{xz} \\ \varepsilon_{yx} & \varepsilon_{yy} & \varepsilon_{yz} \\ \varepsilon_{zx} & \varepsilon_{zy} & \varepsilon_{zz} \end{bmatrix}$$

Tridimensional representation of the strain tensor due to its properties, $\varepsilon_{ij} = \varepsilon_{ji}$

1.2.3 Quasi-static Moduli form Stress-strain Data

The theory of linear elasticity deals with situations where there are linear relationships between applied stresses and resulting strains. The coefficients that related these two properties are called elastic moduli.

This group of elastic moduli is composed by:

Young's modulus (E), Poisson's Ratio (v), Shear Modulus (G), and Bulk modulus (K) the inverse of K (1/K) is known as compressibility.

There are several tests that could be run under quasi-static conditions; all of them try to measure mechanical properties of the rock. This work is interested in the uniaxial compression test, which is the test that was conducted for our samples. In this test, a right circular cylinder of rock (sample) is compressed between two parallel rigid plates. And stress (Load) and strain (deformation) is recorded.

In the uniaxial test, the elastic properties can be characterized by the following relationships:

Young's Modulus (E): or Modulus of Elasticity which is a measure to the stiffness of the sample is:

$$E = \frac{\sigma}{\varepsilon} \qquad \text{..... (1)}$$

Poisson's Modulus (v): or Coefficient of Transverse Deformation which is a measure of the lateral expansion due to longitudinal contraction:

$$\nu = \frac{\varepsilon_{lateral}}{\varepsilon_{axial}} = \frac{\Delta d / d}{\Delta l / l} \quad \text{..... (2)}$$

1.3 Horizontal and vertical direction: Dynamic Measurements

There are some important situations where stresses of a dynamic nature and the propagation of these stresses through the rock as a wave must be considered, some examples of these are: explosive blasting, earthquakes, and rock burst due to excavations.

The resulting stresses and displacements can be analyzed using waves traveling through the rock which are governed by the law of linear elasticity (Seismic waves) (Jaeger *et at*.).

1.3.1 Compression and Shear Velocities

Considering a homogeneous, isotropic and linear elastic material:

Compression Velocity (V_p) is:

$$V_p = \sqrt{\frac{K+4/3G}{\rho}} \quad \text{..... (3)}$$

And the shear velocity (V_s) is:

$$V_s = \sqrt{\frac{G}{\rho}} \quad \text{..... (4)}$$

Where ρ is the density of the material (sand density 2.72 gm/cc).

1.3.2 Dynamic Moduli from Velocities

In the dynamics tests, Young's and Poisson's Modulus is represented by the following equations:

$$\text{(Young's Modulus)} \quad E = \frac{\rho V_s^2 (3V_p^2 - 4V_s^2)}{(V_p^2 - V_s^2)} \quad \ldots\ldots\ldots\ldots (5)$$

$$\text{(Poisson's Modulus)} \quad \nu = \frac{(V_p^2 - 2V_s^2)}{2(V_p^2 - V_s^2)} \quad \ldots\ldots\ldots\ldots\ldots (6)$$

V_s is the velocity of Shear Wave, Vp is the velocity of Compression Waves, and ρ corresponds to the rock density. The others modulus (G and K), could be calculated with the relationships described in Eq.(3),(4) above.

1.4 Effect of Rock Anomalies (Fractures) on Quasi-static and Dynamic Measurements

Fractures in the rock sample are void spaces that can be compressed at a certain load application. Fig. (2) describes three kinds of rock, one with no fractures, one with vertical fractures and the other with horizontal fractures. As expected, the horizontal fractures are easy to compress meanwhile a rock with no fractures is a stiffer sample.

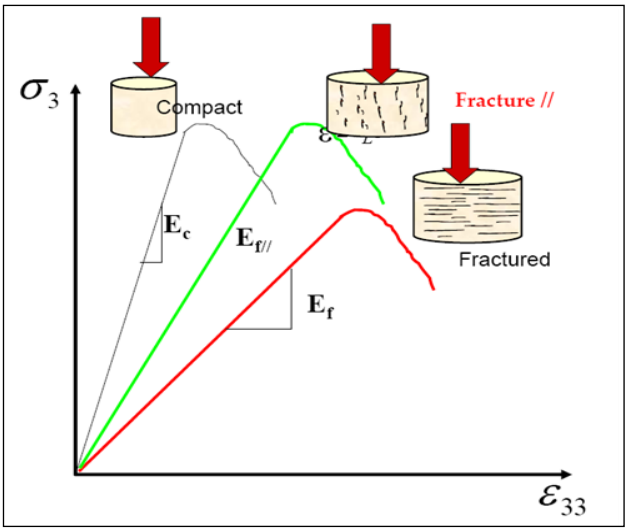

Fig. (2) Berea Sandstone Rock Sample (Source: Dr. Abousleimann Class Notes Fall 2009)

2. Materials Equipment and Procedures

The PoroMechanics Institute (PMI) provided the Berea sandstone core sample and all the required material and equipment for the characterization of the rock elastic parameters.

2.1 Sample Descriptions

Berea sandstone is a medium-grained, Mississippian age graywacke. It is composed of quartz (~80%), feldspar (~5%), clay (predominately kaolinite) (~8%), and calcite (~6%) (Hart, 2000). Its grains are well sorted and sub-angular with quartz overgrowths. An estimate porosity of the Berea sandstone is 20%. The core sample analyzed comes from the Berea Sandstone formation located in Berea town – Oklahoma State, USA. The core sample was taken from the vertical direction of the block rock. Fig. (3) shows the cylindrical core sample.

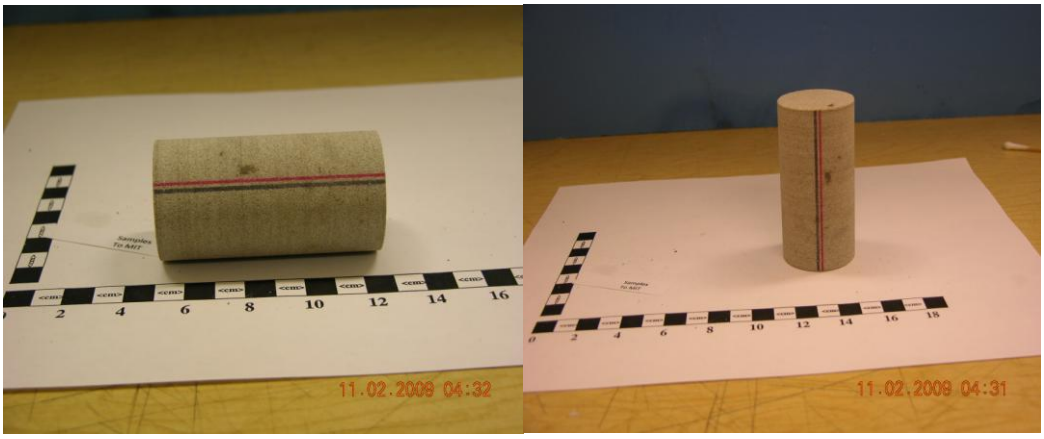

Fig. (3) Berea Sandstone Rock Sample.

The dimensions of the rock sample were measured using a micrometer. The average of 3 measurements is reported in Table (1).

Table (1) Berea Rock Sample Dimensions

Dimension	Magnitude	Units
Length	2.9865	in
Diameter	1.493	in
Area	1.7507	in2

2.2 Sample Preparation

The sample was provided by the PMI laboratory. Berea rock sample were already cored, and ground into right cylinders with dimensions of approximately *2.9865 in.* length and *1.4930 in.* in diameter. Sample has three objectives to acquire the required data for characterization. These objectives are: to attach a strain gauge in the side of the cylindrical sample, to attach an extensometer surrounding the sample, and to attach the crystal at the ends of the cylinder shape sample. Let's start describing one by one. The strain gage (CEA-06-250UN-350) is attached to the sample in order to monitor the Axial

Strain. First, the center axial distance of the sample was marked intersected. In this region a thin layer of epoxy was applied in order to have a smooth surface.

The epoxy was then polished with sand paper until the rock matrix surface was visible.

The rock surface was cleaned with an acidizing conditioner followed by a neutralizer to enhance the effect of the glue which is about to be applied. A thin layer of catalyzer was then added to the surface of the strain gauge. Super glue sticks the gauge in place on the core sample Fig. (4).

Fig. (4) Epoxi preparation and application, Strain gauge attachment procedure.

Now, three wires (which will transmit the deformation changes of the rock/gauge to the computer) are welded to the strain gauge terminals. Fig. (5) shows the rock sample with the strain gauge in place.

To record lateral deformation the extensometer is attached surrounding the circumference of the core sample. The extensometer will record while axial load is being applied. For the dynamic method, acoustic measurements are required. Compression and shear waves traveling through the core are registered and their arrival times are required for the calculation.

For this purpose, crystals are attached to the rock sample.

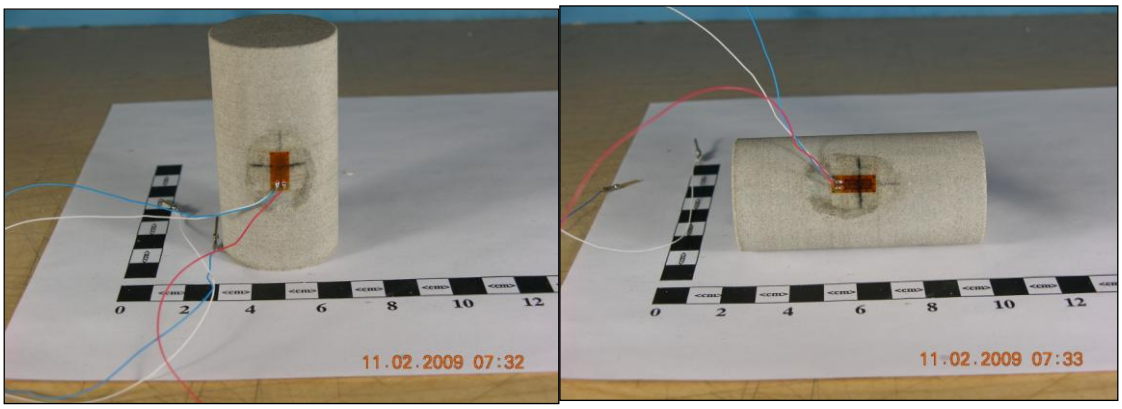

Fig. (5) Strain gauge and three wires after setting on the rock surface.

A set of two crystals go on each side of the core sample in the axial direction and lateral direction. Figure 6 shows the crystals that go on top and bottom of the core (Axial direction). The two crystals shown in Fig.(6) produce compressional waves (thick crystal) and shear waves (thin crystal).

At the other end of the core sample, two crystals are also attached to register the arrival time of the waves emitted by the first. The waves travel first through the metal, second through the rock sample and then again though the metal in the other end. These waves are represented roughly by the red line in Fig.(6), meaning that a

correction has to be applied to obtain the arrival time of the rock only. Further discussion on this is provided in the data acquisition section.

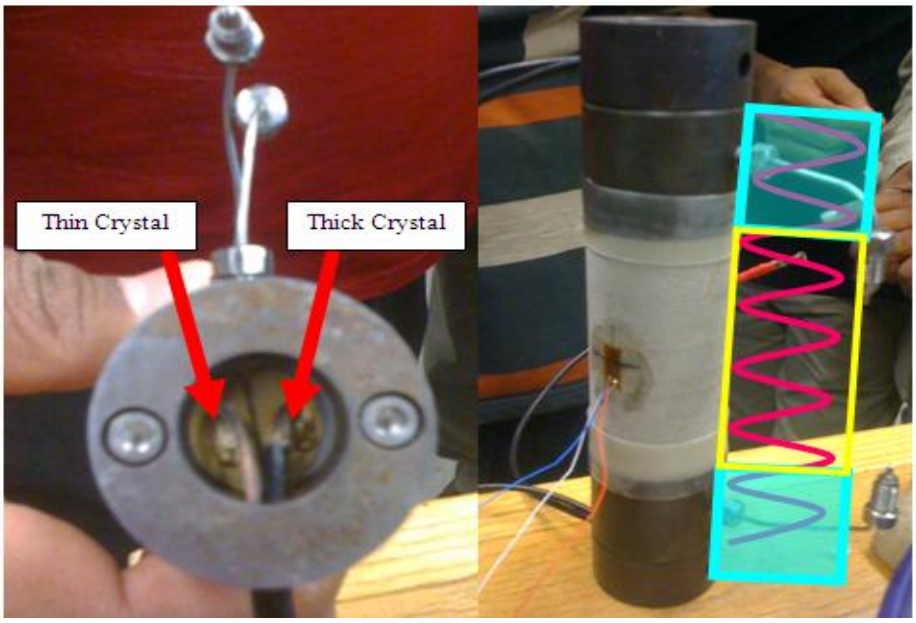

Fig. (6) Crystal attached to the core sample. Axial Direction.

Fig. (7) shows the rock sample already mounted in the MTS and the extensometer around the sample.

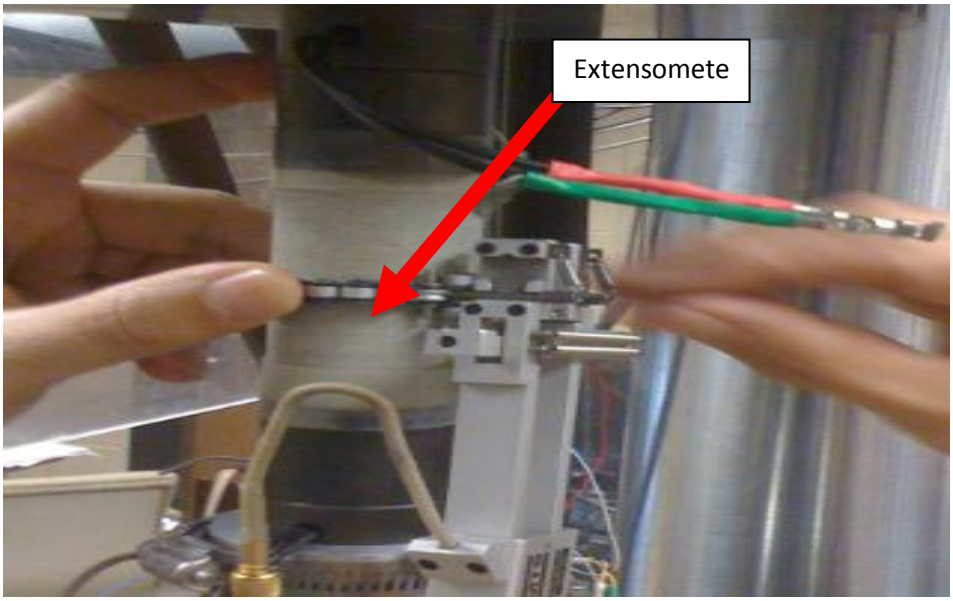

Fig. (7) Rock sample mounted in the MTS with the extensometer around it.

2.3 Testing Frame and Load Application

The test was conducted in the PoroMechanics Institute (PMI) of the University of Oklahoma in Norman, OK. The testing frame description provided here was extracted from the PMI web site. The **MTS 819** load frame is capable of either tensile or compressive loading while simultaneously applying torsional loads to a rock core sample. The apparatus has an operational range of 50 kips force in the tension and compression modes and 20,000 inch pound torsional force. Hydraulic grips are available to accommodate samples up to 2 inch in diameter. The system has a MTS Flex Test SE controller for servo-operation of the system. The load frame has been used with appropriate additional fixtures for direct tension test, Brazilian tension tests, unconfined compession experiments, uniaxial tests, triaxial tests, torsional test of hollow rock cylinders, fracture toughness tests, and fracture growth in plates. Triaxial tests with confining vessel are performed for small size samples at any confining pressure or NX size samples (2 1/8 inch diameter 4 1/4 inch length) with low strength or low confining pressures.

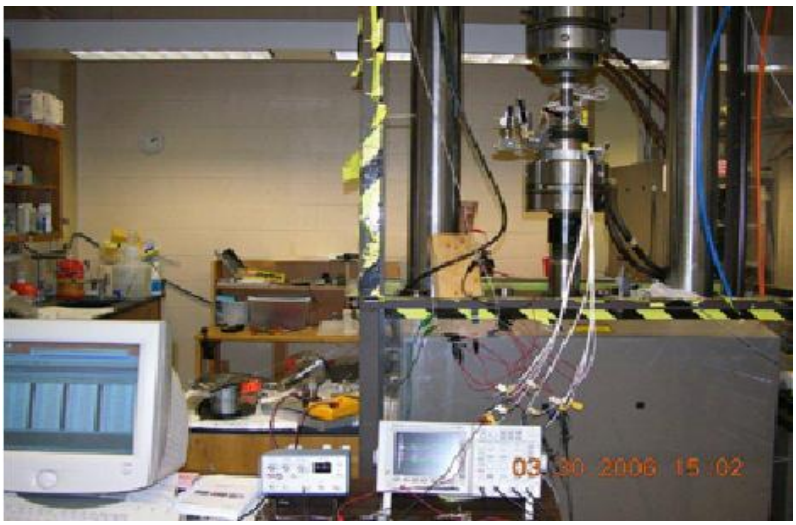

Fig. (8) MTS 819 load frame. MTS Data Acquisition system.

*(*After PMI Website November 2009)

As seen in Fig.(8), the cylindrical core sample is already mounted in the MTS 819 load frame. The strain gage, the extensometer and the crystals are properly connected to transmit the data to the data acquisition system Fig.(9) Uniaxial load is applied continuously to the core sample. Meanwhile this load is applied, all the sensors connected to the rock start to register the changes in the rock itself. The strain gage and the extensometer register the changes in length and diameter of the sample.

Meanwhile the crystals attached to the sides of the rock register the time that the compression and shear waves take to travel through the core in the axial and lateral direction.

Fig. (9) MTS 819 load frame. Rock sample mounted in the MTS 819. MTS Data Acquisition system. (After PMI Website November 2009*)*

2.4 Data Acquisition

After mounting the sample and connecting properly all the measurement equipment, the MTS 819 load frame starts applying load. While the strain gage and the extensometer register the behavior of the rock continuously, the arrival times of the compressional and shear wave are to be recorded at given loads. This loads were determined to be 0, 3500, 7050, 10500, 16640 lbf. These 5 measurements provide a mid-point arrival time used to calculate the Young's Modulus and the Poisson's Ratio using the dynamic method.

The strain gage and the extensometer provided 2148 data points each. The range of load went from *0* to *14590 lbf*. At that load the rock failed. A plot of stress vs. strain is obtained and from there the Young's Modulus and Poisson's Ratio can be derived.

For the dynamic method, measurements of the compressional and shear wave arrival time were registered. Fig. (10) shows the plot

of deviatory compressional wave vs. wave arrival time. This arrival time means, the time it takes the wave to reach the other crystal. Fig.(10) is showing the time it takes the wave to travel through the metal only. No core sample was put in between the platens containing the crystals. From fig.(10), the time it takes the compressional wave to travel through the metal is approximately *10.6 μs*.

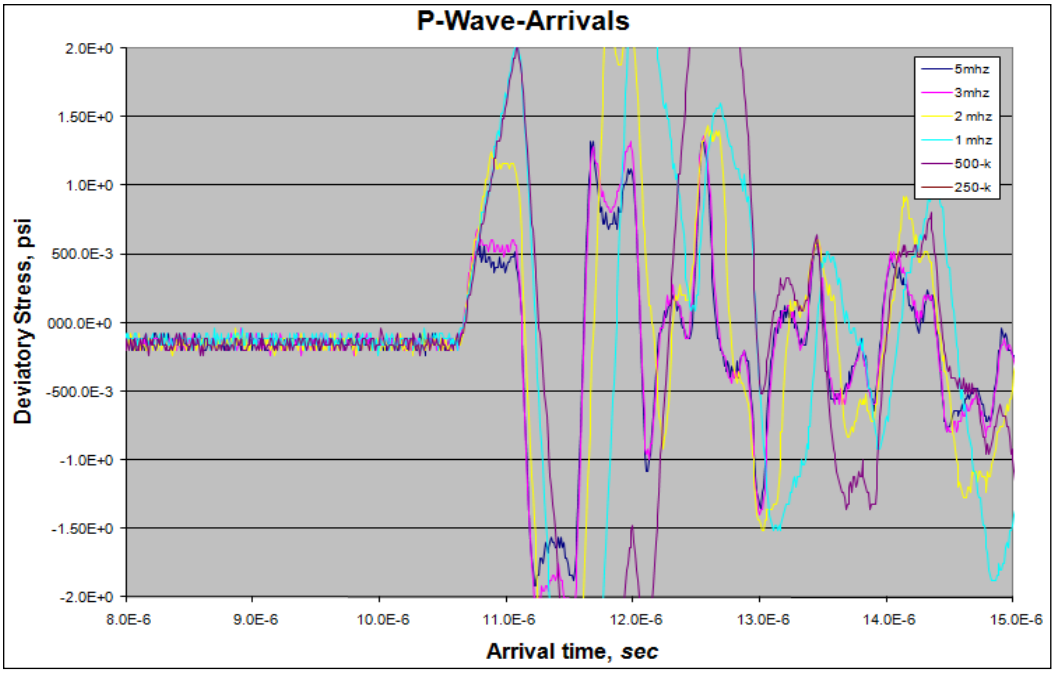

Fig. (10) Compressional wave arrivals

Also:

Fig.(11) was obtained measuring the time it takes the wave to travel through the platens only. Fig. (11) shows the plot of deviatory shear wave vs. wave arrival time. From fig. (11), the time it takes the shear wave to travel through the metal is approximately *20.1 μs*. These arrival times, *10.6 us* and *20.1 us*, for compressional and shear waves respectively, are to be used as correction factors once the rock sample is in between the platens.

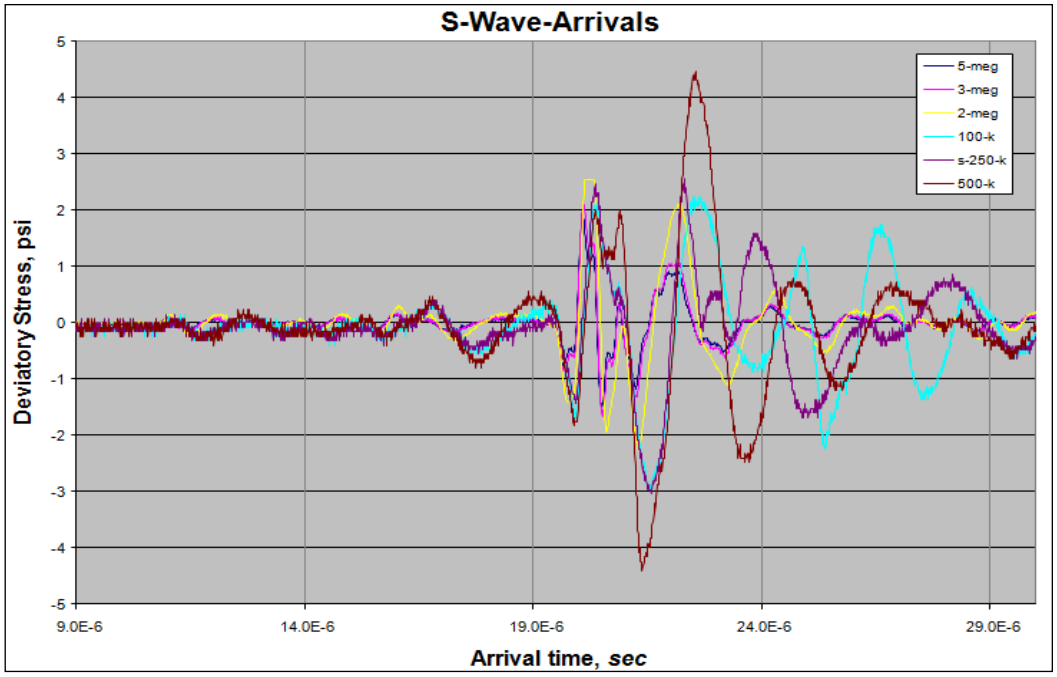

Fig. (11) Shear wave arrivals

As mentioned before, measurements of wave arrival times are recorded at 5 different load during the core loading test. The following figures show the plot obtained at 1 of the 5 load recorded. More specifically, the data registered at *7050 lbf* load is displayed in these figures. Fig.(12), shows the axial compressional wave behavior traveling from one crystal to the other passing through the rock sample in between. The arrival time is easy to read compared to the shear wave plot.

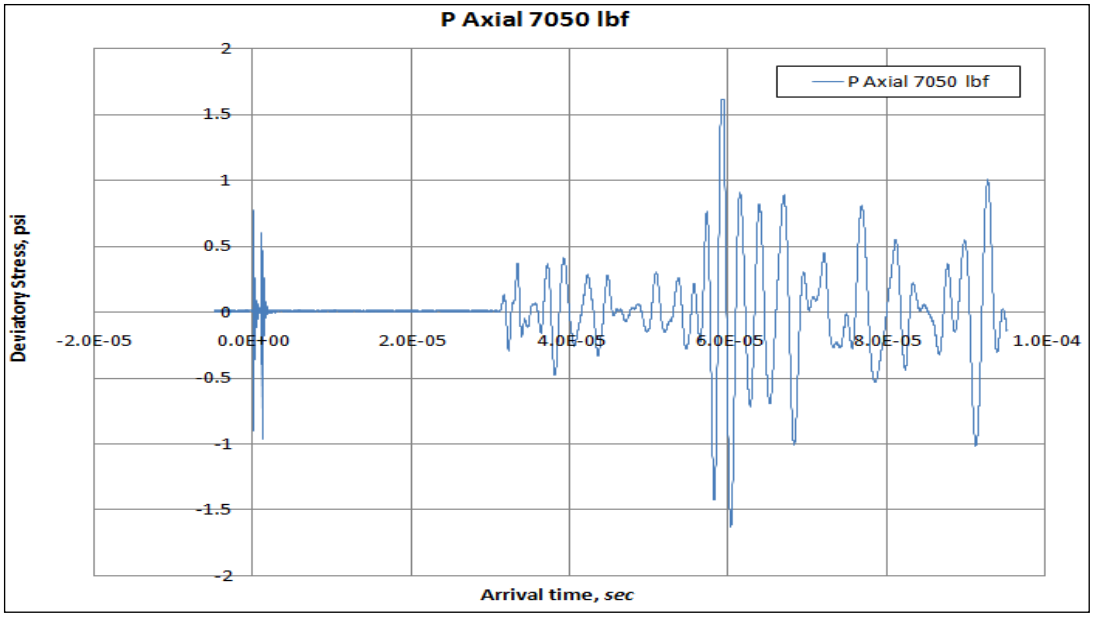

Fig. (12) Axial compressional wave arrival time at 7050 Lbf load.

In this case, for figure PA, the arrival time is approximately 30.5 μs. This arrival time considers the rock sample and the metal in both ends. By subtracting the correction time *10.6* μs (Obtained from fig.(10) to 30.5 μs, the travel time though the rock is obtained. Therefore, it takes 19.9 μs for The compressional wave to travel through the rock sample.

For the shear wave travel time through the rock sample, the same procedure is carried. But this time, it is a little bit more difficult to read the arrival time from fig. (13). This is because, shear waves also produce compressional wave when they are released. This means that in the plot both waves are plotted. The challenging issue is to identify correctly one versus the other. For example, in figure SA, the arrival time of the compressive wave is clearly identified as 30.5 μs.

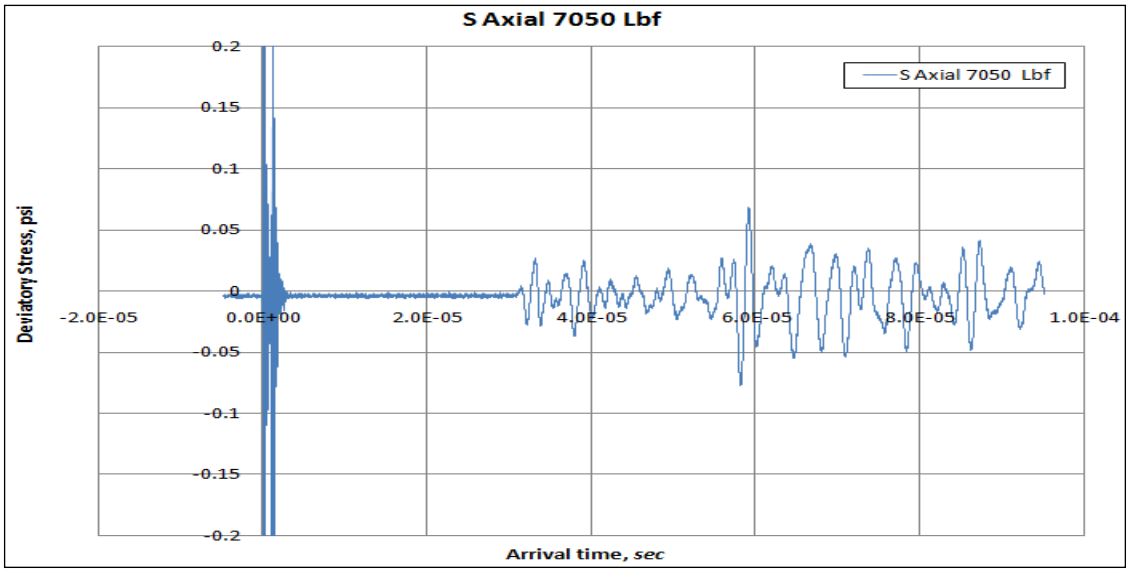

Fig. (13) Axial shear wave arrival time at 7050 Lbf load

Now, it will take the shear wave approximately double that time to get to the other end. In that context, a wave shape has to be targeted around ~60 μs. If noticed carefully, a wider wave is present at 58.8 μs.

That is most likely the reading of the shear wave arrival time, Once again, this arrival time considers the metals and the rock sample. In order to obtain the travel time through the rock sample a correction is needed,The same procedure as for the compressional wave is applied figs. (14-15).

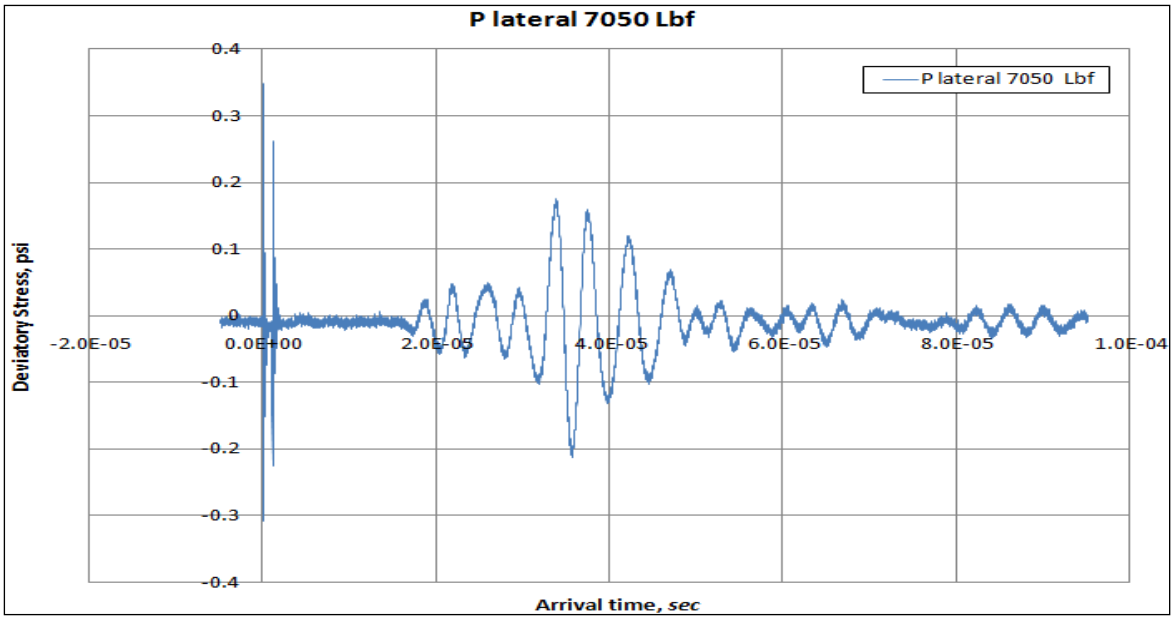

Fig. (14) Lateral compressional wave arrival time at 7050 Lbf load.

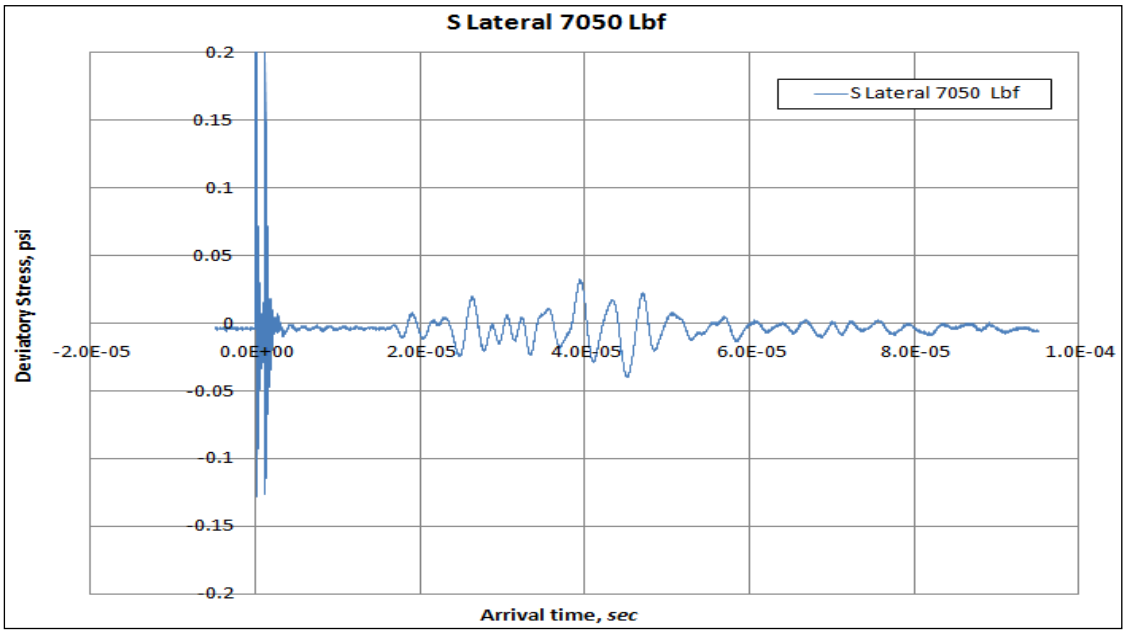

Fig. (15) Lateral shear wave arrival time at 7050 Lbf load.

As mentioned initially, the plot displayed here are only for 7050 LBf load. Table (2) collects all the readings of arrival times at each load step. Table (3) shows the correction factor obtained from Fig.(10),(11).

Table (2) Uncorrected Arrival times of P and S waves.(Axial and lateral direction)

Load, Lbf	Axial Direction		Lateral Direction	
	Compressional P Wave	Shear S Wave	Compressional P Wave	Shear S Wave
	Arrival time, μs	Arrival time, μs	Arrival time, μs	Arrival time, μs
0	42.5	78.4	19.2	50.4
3500	31.5	58.5	18.2	38.1
7050	30.5	58.8	17.9	38.3
10500	30.9	58.5	17.8	38.1
16640	29.9	59.0	19.6	39.3

Table (3) Correction time for P and S waves.(Axial and lateral direction)

	Axial Direction	Lateral Direction
	Time Correction, μs	Time correction, μs
Compressional Wave P Crystal	10.6	6.14E-07
Shear Wave S Crystal	20.1	6.48E-07

Table (4) is obtained after the application of the corresponding correction times.

Table (4) Corrected Arrival times of P and S waves. (Axial and lateral direction)

Load, Lbf	Axial Direction		Lateral Direction	
	Compressional P Wave	Shear S Wave	Compressional P Wave	Shear S Wave
	Arrival time, μs	Arrival time, μs	Arrival time, μs	Arrival time, μs
0	31.9	58.3	18.6	49.8
3500	20.9	38.4	17.6	37.5
7050	19.9	38.7	17.3	37.7
10500	20.3	38.4	17.2	37.5
16640	19.3	38.9	19.0	38.7

3. Results and Discussions

3.1 Results

Now the data that is acquired the proper calculations are made and the wanted results to characterize the rock sample are presented in this section.

3.1.1 Quasi-Static Measurements

Once the loading of the sample started, continuous values for strain and stress were recorded. The strain gage and the extensometer provided 2148 data points each. The range of load went from *0* to *14590 lbf*. Fig. (16) shows the plot of these values.

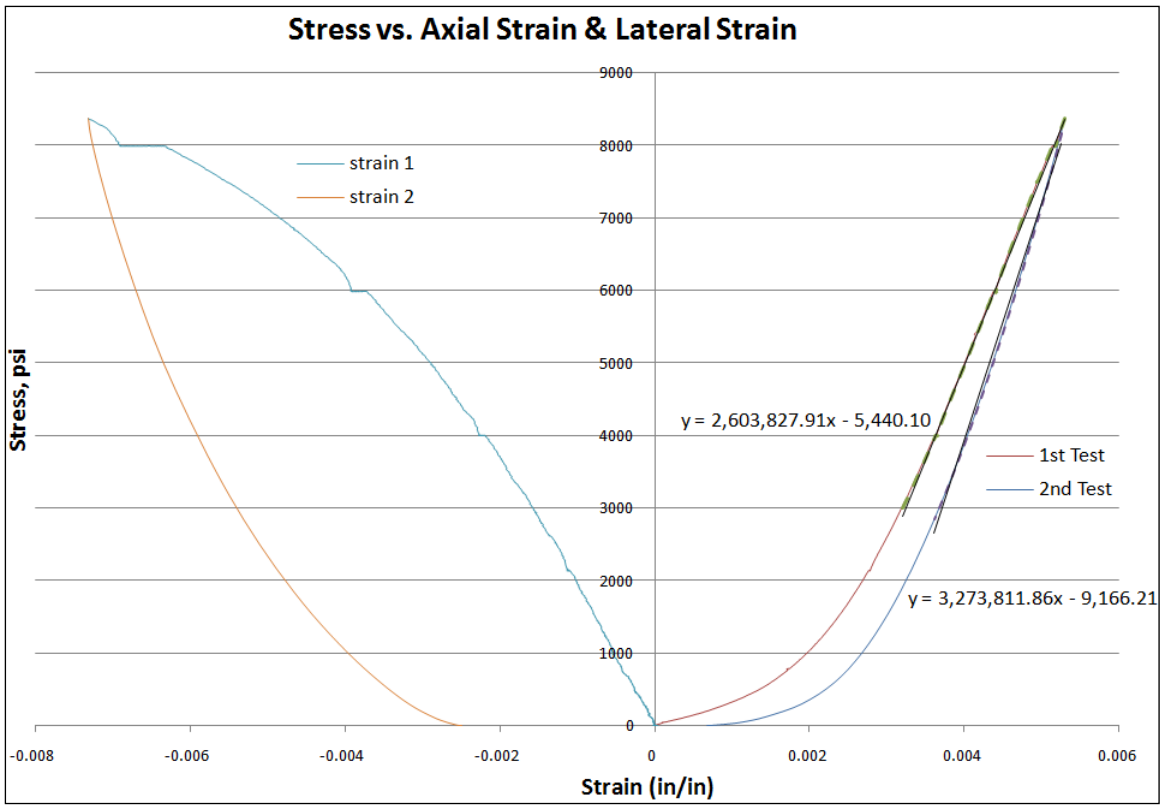

Fig. (16) Stress-strain curve for Berea Sandstone showing Young's modulus (slope) of 2,600,000 psi and 3,200,000 psi.

Notice that two slopes are displayed in the stress vs. strain plot. This is because the loading of the rock had to be stopped for security reasons. More specifically, the load was applied without the control program. After this issue was solved, the rock was loaded again until it failed. It is interesting to notice that in the first loading attempt, the rock Young's modulus of the rock is around 2,600,000 psi and in the second loading attempt, the young's modulus increases to 3,200,000 psi. The difference in the Young's Modulus suggests that the rock sample has been already compressed in during the first attempt making it stiffer. So, it was expected to have a stiffer rock during the second loading attempt. Table(5) shows the Young's Modulus and the Poisson's ratio.

Table (5) Young's Modulus and Poisson's Ratio

Loading Attempt	Young's Modulus	Poisson's Ratio
1st (Upper Curve)	E = 2.6 E 6 psi	
2nd (Lower Curve)	E = 3.2 E 6 psi	V = 0.13

Since the core was loaded up to 9000 Psi without reaching the failure criteria the graphs show a straight line from about 3000 psi up to the end, the slopes and equations are shown along with the R^2=0.98 which indicates how well does the slope fit the data. The lateral strain shows a little noise, this may be due to the sensitivity of the extensometer, creating a less smooth curve.

The Berea sandstone sample failed at more than *14600* lb_f of load. Fig. (17) and (18) show the rock after the failure.

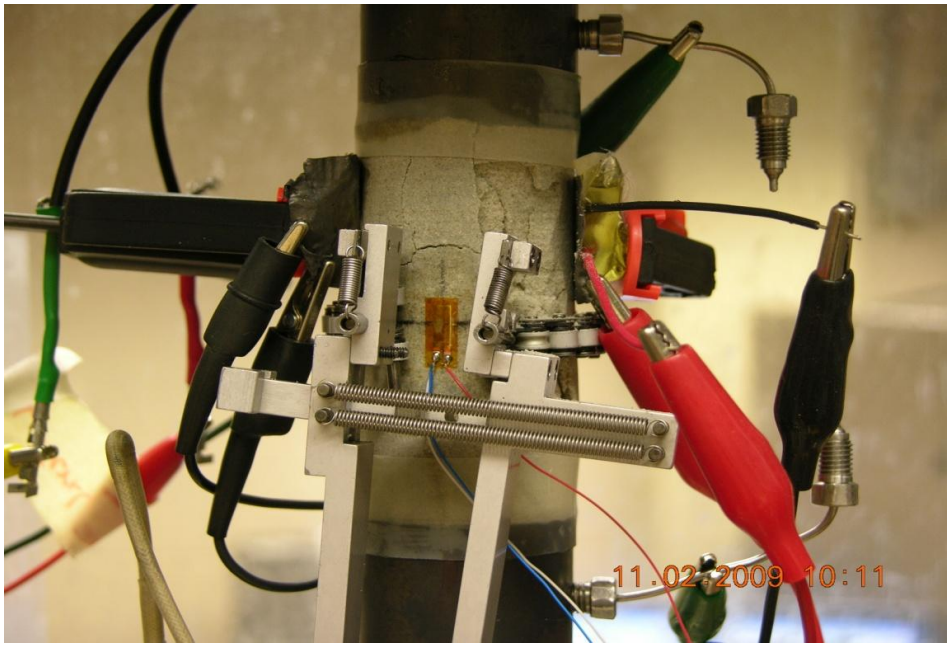

Fig. (17) Berea Sandstone Sample after Failure

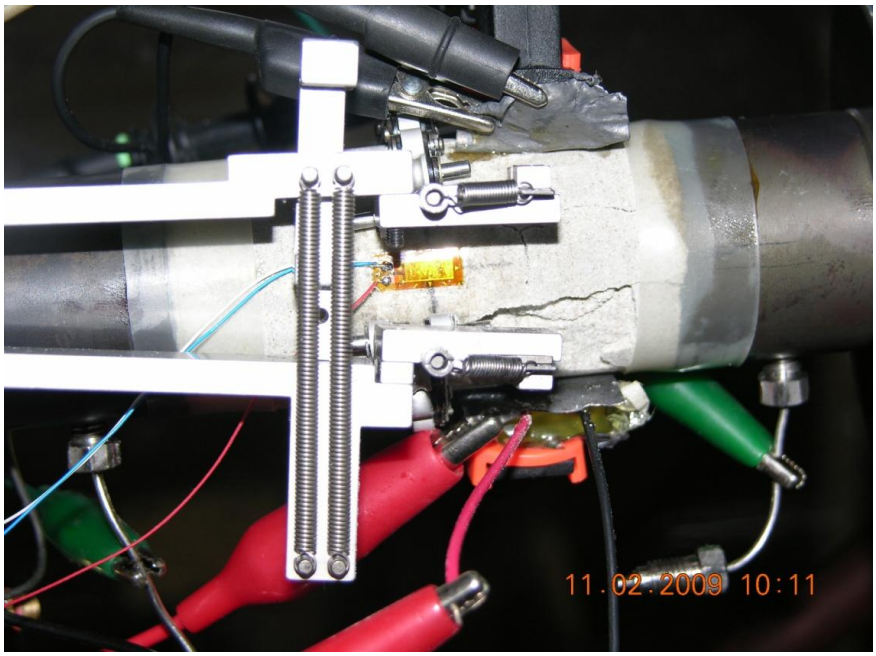

Fig. (18) Berea Sandstone Sample after Failure.

3.2 Dynamic Measurements

Having highlighted the difference in the loading attempts, all the dynamic measurements are registered during the second loading attempt.

3.2.1 Measured Velocities

Table (4) shows the times that the waves took to travel through the rock. Since we know the length and diameter of the Berea core sample, the velocities can be obtained. These values are shown in table(6).

Table (6) P and S waves velocities. Axial and lateral direction.

Load, Lbf	Axial Direction		Lateral Direction	
	Compressional P Wave	Shear S Wave	Compressional P Wave	Shear S Wave
	velocity, m/s	velocity, m/s	velocity, m/s	velocity, m/s
0	2378.0	1301.2	1975.1	752.4
3500	3629.5	1975.4	4168.0	995.3
7050	3811.9	1960.1	4237.8	990.1
10500	3736.8	1975.4	4261.6	995.3
16640	3930.4	1950.1	3870.3	964.9

Notice that the compressional wave velocity in the axial direction has an increasing pattern as the load increases. The explanation for this effect is as follow. The load applied to the sample compresses the rock. The contact between the grains in the rock increases due to compression. Since there is more grain contact, the sound waves travel faster from one point to the other inside the rock matrix leading to higher velocities.

3.2.2 Computed Dynamic Moduli

Young's Modulus and Poisson's Ratio can be obtained by substituting the values given in Table (3) then using Eq. (5), (6). Table (7) and (8) present the calculated values for Young's Modulus and Poisson's ratio, respectively.

Table (7) Poisson's Ratio for different loads.

Load, Lbf	Axial Direction	Lateral Direction
	Poisson's Ratio	Poisson's Ratio
0	0.286	0.415
3500	0.290	0.470
7050	0.320	0.471
10500	0.306	0.471
16640	0.337	0.467

Table (8) Young's Modulus for different loads.

Load, Lbf	Axial Direction	Lateral Direction
	Young's Ratio	Young's Ratio
0	1.72E+06	6.32E+05
3500	3.97E+06	1.15E+06
7050	4.00E+06	1.14E+06
10500	4.02E+06	1.15E+06
16640	4.01E+06	1.08E+06

For comparison purposes, all the information is grouped by direction. The result is shown in table (9).

Table (9) Dynamic measurements and calculations. Axial direction.

LOAD	Stress, psi	Vp (m/s)	Vs (m/s)	E (psi)	v
0	0.00	2378.0	1301.2	1.72E+06	0.286
3500	1999.21	3629.5	1975.4	3.97E+06	0.290
7050	4026.98	3811.9	1960.1	4.00E+06	0.320
10500	5997.63	3736.8	1975.4	4.02E+06	0.306
16640	9504.82	3930.4	1950.1	4.01E+06	0.337

Fig. (19) is a plot of the compressional and shear axial velocities change while the load changes.

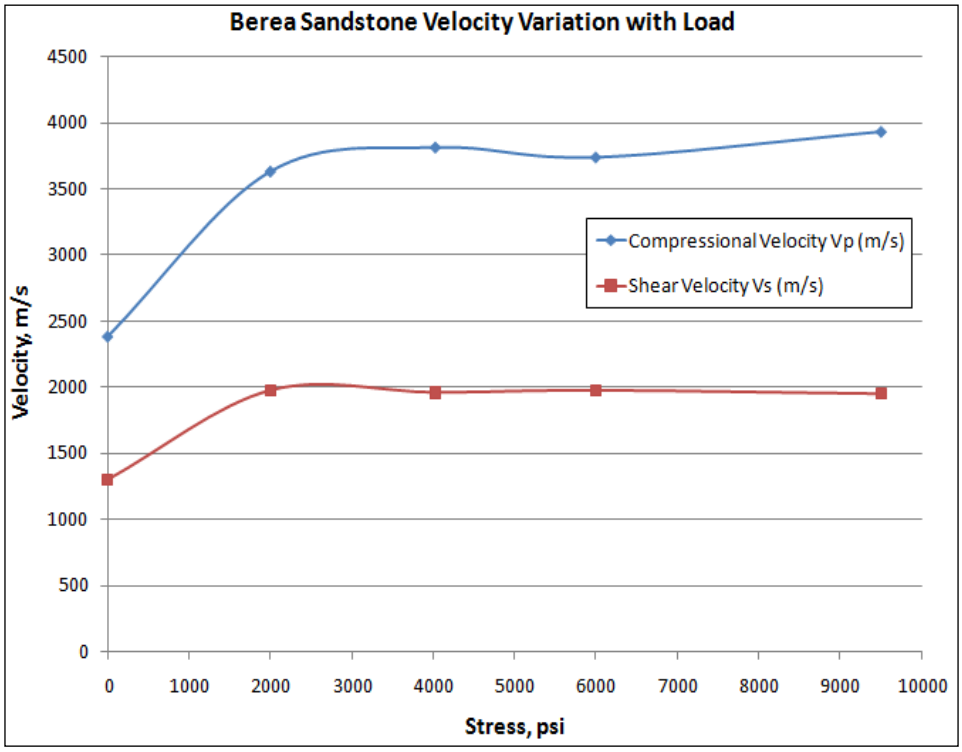

Fig. (19) Compressional and shear axial velocities change while loading.

Now, the information of the lateral is shown in table (10).

Table (10) Dynamic measurements and calculations. Lateral direction.

LOAD	Stress, psi	Vp (m/s)	Vs (m/s)	E (psi)	v
0	0.00	1975.1	752.4	6.32E+05	0.415
3500	1999.21	4168.0	995.3	1.15E+06	0.470
7050	4026.98	4237.8	990.1	1.14E+06	0.471
10500	5997.63	4261.6	995.3	1.15E+06	0.471
16640	9504.82	3870.3	964.9	1.08E+06	0.467

Fig. (20) is a plot of the compressional and shear lateral velocities change while the load changes.

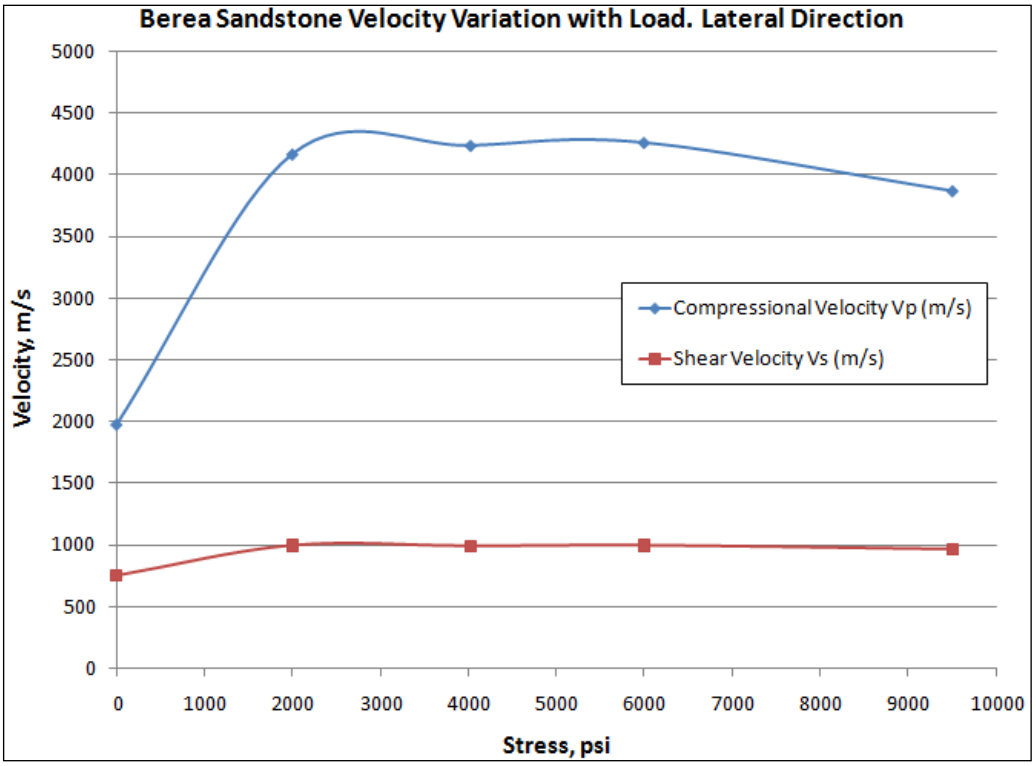

Fig. (20) Compressional and shear lateral velocities change while the load.

3.3 Discussions of Results

In the vertical sense, the quasi-static test results showed a Young modulus is 3200000 Psi. Also, we noted during the experiment that the straight line (as shown in Fig.(16)), start to decline at 9000 Psi. This decline at this value is evidence that the sample starts to faller; therfore we got the Young modulus for the core sample before the core is destroed. The Poisson's ratio was 0.13. The results from table (6), show an increase in the Young modulus with the increase in load, which is the normal expected behavior since at a higher compression the grains become closer to each other and further deformation is reduced, the difference between the calculations for the two types of crystals settings (lateral and axial). Therefore, we observed that the axial measurement is the most reliable, since the end platens are always in the same place and we apply the higher load directly on the core sample and the wave through the core sample will be better. For the lateral test we can use limited load during the experiment, and always lower load value.

4. Conclusions

After analyzing the Berea Sandstone rock sample, the results are consistent with the previous work done in this formation. The rock sample had a slightly elastic behavior as shown in the results of our quasi-static test. The quasi-static test shows an initial incline behavior and then a straight line meaning an elastic behavior at that loading

interval. Unlike other Berea samples, this one seems to be more consolidated (different cores for other wells).

5. Nomenclature:

E	Young's modulus
V	Poisson's Ratio
G	Shear Modulus
K	Bulk modulus
σ	Stress
ε	Deformation
ρ	Density of the material
V_s	The velocity of Shear Wave
Vp	The velocity of Compression Waves

6. Bibliography and List of References

1. Abousleiman, Y. "Geomechanics in Integrated Reservoir Characterization I" Reservoir Characterization I. University of Oklahoma Class presentation, Norman. Oklahoma. Fall 2009.
2. Coates, D.F. "Rock Mechanics Principles" Monograph 874 Canadian Centre for Mineral and Energy Technology, Ottawa, Canada 1981.
3. David J. Hart, "Laboratory measurements of poroelastic constants and flow parameters and some associated phenomena," University of Wisconsin, Madison, 2000.
4. Fjaer, E. Holt, R.M., Horsrud, P. Raaen, A.M., Risnes, R. "Petroleum Related Rock Mechanics", First Edition, Developments in petroleum science 33. Elsevier, Amsterdam, the Netherlands, 1992.
5. Sierra, Velazquez, Libreros, Cless, "The Geomechanics and the Acoustic Anisotropy of Rocks from Hollywood Quarry Arkansas", Laboratory Project Report. GEOL 6970, Fall 2008.